Quaternary Science Reviews 129 (2015) 308–320

Contents lists available at ScienceDirect

Quaternary Science Reviews

journal homepage: www.elsevier.com/locate/quascirev

On the timing and forcing mechanisms of late Pleistocene glacial terminations: Insights from a new high-resolution benthic stable oxygen isotope record of the eastern Mediterranean

T.Y.M. Konijnendijk*, M. Ziegler, L.J. Lourens

Utrecht University, Faculty of Geosciences, Institute for Earth Sciences, Budapestlaan 4, 3584 CD, Utrecht, The Netherlands

ARTICLE INFO

Article history:
Received 9 April 2015
Received in revised form
5 August 2015
Accepted 1 October 2015
Available online 4 November 2015

Keywords:
Pleistocene
Benthic isotopes
Stratigraphy
Mediterranean
Astronomical tuning

ABSTRACT

Benthic oxygen isotope records of deep marine sedimentary archives have yielded a wealth of information regarding ice sheet dynamics and climate change during the Pleistocene. However, since they often lack independent age control, these records are generally bound by a fixed phase relationship between orbital forcing and the climate response, e.g. ice volume changes. We present the first long (~1.2 Ma) benthic oxygen isotope record from the eastern Mediterranean, based on ODP Sites 967 and 968, which clearly reflects the behavior of global climate on a glacial–interglacial scale throughout the late Pleistocene time period. The age model for our record is based on tuning the elemental ratio of titanium versus aluminum (Ti/Al) against insolation. The Ti/Al record is dominated by the precession-related changes in northern African climate, i.e. monsoonal forcing, and hence largely independent of glacial–interglacial variability. We found the largest offset between our chronology and that of the widely applied, open ocean stacked record LR04 (Lisiecki and Raymo, 2005) for T_{VII} (~624 ka), which occurred ~9 kyr earlier according to our estimates, though in agreement with the AICC2012 δD_{ice} chronology of EPICA Dome C (Bazin et al., 2013). Spectral cross-correlation analysis between our benthic $\delta^{18}O$ record and 65°N summer insolation reveals significant amounts of power in the obliquity and precession range, with an average lag of 5.5 ± 0.8 kyr for obliquity, and 6.0 ± 1.0 kyr for precession. In addition, our results show that the obliquity-related time lag was smaller (3.0 ± 3.3 kyr) prior to ~900 ka than after (5.7 ± 1.1 kyr), suggesting that on average the glacial response time to obliquity forcing increased during the mid-Pleistocene transition, much later than assumed by Lisiecki and Raymo (2005). Finally, we found that almost all glacial terminations have a consistent phase relationship of ~45 ± 45° with respect to the precession and obliquity-driven increases in 65°N summer insolation, consistent with the general consensus that both obliquity and precession are important for deglaciation during the Late Pleistocene. Exceptions are glacial terminations T_{IIIb}, T_{36} and potentially T_{32} (and T_{VII} T_{24} and T_{34}), which show this consistent phase relationship only with precession (only with obliquity). Our findings point towards an early (>1200 ka) onset of the Mid Pleistocene Transition. Vice versa, the timing of T_{VII}, which can only be explained as a response to obliquity forcing, indicates that the transition lasted until at least after MIS 15.

1. Introduction

The global climate state shifted through the past 1 million years (Myr) of Earth's history from a predominantly obliquity driven glacial–interglacial mode towards a pronounced 100-kyr glacial–interglacial rhythm (Imbrie et al., 1993; Tiedemann et al., 1994; Lisiecki and Raymo, 2005). This transition is known as the Mid Pleistocene Transition (MPT) and its origin is still under debate (e.g Clark et al., 2006; Maslin and Ridgewell, 2005). Part of the discussion relates to the fact that the benthic foraminiferal $\delta^{18}O$ isotope record – reflecting both changes in deep sea water temperatures and the isotopic composition of sea water through the uptake of isotopically light water in ice sheets – behaves inconsistently with respect to the astronomical cycles of precession and obliquity, which are considered as the major forcing mechanisms of the glacial–interglacial variability during this time period (Hays

* Corresponding author.
E-mail address: T.Y.M.Konijnendijk@uu.nl (T.Y.M. Konijnendijk).

http://dx.doi.org/10.1016/j.quascirev.2015.10.005

et al., 1976; Imbrie et al., 1993; Tiedemann et al., 1994; Lisiecki and Raymo, 2005). The available knowledge of how climate and ice sheets respond to the precession and obliquity-driven insolation usually stems from the last and penultimate glacial–interglacial transitions, which are well constrained by highly detailed records that are readily datable using radiocarbon or other absolute methods (e.g. Lourens et al., 1996; Martrat, 2004; Lemieux-Dudon et al., 2010). This inferred knowledge about climate response to insolation forcing has generally been extrapolated into the past. In other words, a predefined relationship is used to tune the benthic foraminiferal $\delta^{18}O$ isotope record to insolation forcing using a fixed phase lag between the data and the target curve, generally represented by a simple ice-sheet model (e.g. Shackleton et al., 1990; Lisiecki and Raymo, 2005).

With the availability of long and high quality records, Lisiecki and Raymo (2005) established a state of the art marine isotope chronology based on 57 benthic isotope records, spanning the last 5.3 Ma: the LR04 benthic oxygen isotope stack. This high-resolution reconstruction of global climate is the current global standard for correlating marine isotopic records as well as many other climate reconstructions (e.g. Bintanja et al., 2005; Wolff et al., 2006; Parrenin et al., 2007; Tzedakis, 2007). The age model for the LR04 benthic stack was established by tuning the linear components to a simple ice sheet model (Imbrie and Imbrie, 1980). In this model it is assumed that the phase lags in ice sheet response at the frequencies of obliquity and precession are those of a single exponential system (Imbrie and Imbrie, 1980; Imbrie et al., 1984; Lisiecki and Raymo, 2005). The ice-sheet model (1) is forced by the 21 June 65°N insolation curve (Laskar et al., 1993; 'x' in equation (1)), taking into account an ice sheet response time (Tm) of 15 kyr and a non-linearity coefficient b of 0.6. These values are based on radiometric dating of the penultimate glacial cycle (Imbrie and Imbrie, 1980) and kept constant for the last 1500 kyr (Lisiecki and Raymo, 2005).

$$dy/dt = (1 \pm b)/Tm\,(x - y) \quad (1)$$

The change in ice volume over time (dy/dt) therefore depends on the insolation forcing × versus present ice volume y, with nonlinearity constant b switching signs: it is negative while ice is growing and positive when the ice sheets decay (i.e. when dy/dt is negative). Together this describes the slow buildup and fast ablation of the ice sheets with a delay in ice sheet response of 4.2, 5.0 and 7.9 kyr in the 19 and 23 kyr components of precession and the 41 kyr component of obliquity, respectively. The constants Tm and b are generally assumed to be invariant with time even though the accumulation rate and size of the ice sheet varied continuously (Shackleton et al., 1990). One objection to the above methods is that we have insufficient possibilities to verify the outcome of such tuned age models. In a limited number of cases a reversal of the earth's magnetic field or radiometrically datable tephra layers generates some control on the tuning, but in most situations the astronomical age model is more precise and deviations fall within error margins of possible secondary age control (Shackleton et al., 1990). Lisiecki and Raymo (2005) used sedimentation rate as a control on their age model. They labored under the reasonable assumption that their stack cannot exhibit overly large variations in sedimentation rate. Therefore, they restrict the algorithm's freedom to compress or stretch their record in tuning it to insolation. This conservative approach however still overrides any natural variability in system earth's response to insolation forcing by aligning the record to a model with predefined response times.

The broadly accepted astronomically-based tuning approach was tested by Huybers and Wunsch (2004), who used only sedimentation rate as an estimate with radiometrically dated geomagnetic boundaries as age markers. With this approach they produced independent age constraints for isotopic shifts, and argued that tuning to insolation suppresses weak non-linear interactions, i.e. climate variability with periodicities of 70 and 29 kyr. Also, the role of eccentricity-modulated precession is often criticized, with obliquity suggested as the dominant late Pleistocene climate forcing (Huybers and Wunsch, 2004; Maslin and Ridgewell, 2005; Huybers, 2007, 2011). Note that late Pleistocene is used here to express the last ~900 kyr, whereas 'early Pleistocene' indicates the period before 900 ka (contrast the Late Pleistocene, formally defined to be 0–125 ka; Gradstein et al., 2004). Unfortunately, letting sedimentation rates dictate the age model entirely introduces large uncertainties in the estimates. Adding a different form of age control is the best way to improve this valuable approach.

Better estimates of the phase relation between insolation forcing and the benthic $\delta^{18}O$ response are necessary to improve our understanding of the timing and nature of climatic shifts, such as the MPT and glacial terminations. Outside the realm of deep sea coring there is a variety of settings offering the possibility of climate reconstruction, sometimes with the advantage of additional age control, like radiometric dating. Reconstructions of sea level in relation to ice volume changes have been based on the coral reef growth of Barbados (Harmon et al., 1978, 1983; Bard et al., 1990) using ^{14}C dating and U/Th dating for the last 250 kyr. Dutton et al. (2009) used a set of U/Th-dated speleothems from Italy to reconstruct the sea level of MIS 7 in detail. Also of very high resolution is the speleothem-derived monsoon activity reconstruction of Sanbao-Hulu (Wang et al., 2008; Cheng et al., 2009). The speleothem $\delta^{18}O$ record reflects changes in the strength of the East Asian summer monsoon. The record is dated by U/Th dates back to ~390 ka with average dating errors within ~0.5 kyr (Cheng et al., 2009). It is a highly precise, highly accurate paleoclimate record displaying fast climate shifts such as the Dansgaard-Oeschger millennial scale variability, with rapid transitions between stadial and interstadial periods (Wang et al., 2008; Cheng et al., 2009).

While all of these reconstructions provide valuable insights in paleoclimate behavior over the course of the Pleistocene, they lack some of the benefits typical for deep sea coring. The sea level reconstructions based on corals and speleothems depend on specific finds of suitable archives. Such climate archives often only cover a limited time period, which makes these reconstructions discontinuous. The ice core records, while providing detailed and long sequences of paleoclimate, mostly reflect local circumstances like temperature (Jouzel et al., 2007). The Sanbao-Hulu speleothem record reflects the East Asian Monsoon. Neither of these provides an integrated signal of global climate, as it is provided by benthic $\delta^{18}O$ (Hays et al., 1976; Imbrie et al., 1984). In this study we present the first high resolution, long-term (1.2 Myr) benthic oxygen isotope record from the eastern Mediterranean. Our record is uniquely located in a setting that allows us to date the record without tuning the isotopes to insolation or a reference curve. We arrive at our chronology by tuning a geochemical signature of the sediment directly to insolation. Therefore, no assumptions for the response time of ice volume to insolation are required. This approach builds upon earlier work by Ziegler et al. (2010), who reconstructed the last 350 kyr using sediments from ODP Site 968. With this non-standard age model we test the age and duration of all the major isotopic stages and transitions of the last ~1.2 Ma.

2. Materials and methods

2.1. ODP sites 967 and 968

Our study uses data from the adjacent ODP Sites 967 and 968 in

the eastern Mediterranean. ODP Site 967 (34°04′N, 32°43′E) was drilled south of Cyprus, near the Eratosthenes seamount at a water depth of 2554 m. ODP Site 968 (34°20′N, 32°45′E) was drilled on the Eratosthenes seamount at a water depth of 1961 m (Emeis et al., 1996). The data of the two sites have been combined into a single splice using color reflectance data (Konijnendijk et al., 2014). This enabled us to extend the paleoclimatic record of Ziegler et al. (2010) of ODP Site 968, the stratigraphic recovery of which is incomplete further back in time. The construction of the combined splice is described in detail in Konijnendijk et al. (2014). The combined splice of ODP 967 and 968 was sampled at 2 cm intervals. Samples were split into a 3–5 g part that was used for X-Ray Fluorescence (XRF) analysis and the remaining 12–20 g which was washed and sieved for the extraction of foraminifers.

2.2. Stable isotopes

In order to generate a benthic foraminiferal oxygen isotope record for the top 350 kyr, Ziegler et al. (2010) used different species, as no single species was present throughout the whole record. The species that were analyzed are *Gyroidina altiformis*, *Gyroidina neosoldanii*, *Cibicides kullenbergi*, *Hoeglundina elegans*, *Cibicides ungerianus*, and *Melonis pompilianus*. The oxygen isotope data of *H. elegans* were corrected for its enrichment (0.78‰) relative to equilibrium calcite (Grossman, 1984). For the record below 350 ka, i.e. the new data presented here, only the species *G. neosoldanii* and *G. altiformis* were used. Between 2 and 4 specimens were hand-picked from the fraction >212 mm and used integrally for Isotope Ratio Mass Spectrometry (IRMS).

The stable isotope data of the entire record were measured on a Thermo-Finnigan MAT253 mass spectrometer, coupled with a Kiel III automated carbonate reaction device. A standard run consisted of 35 samples interspersed with 3 in-house standards (NAXOS) as well as 8 international carbonate standards (NBS-19). Calibration revealed an analytical precision better than 0.1‰ and 0.03‰ for $\delta^{18}O$ and $\delta^{13}C$, respectively.

2.3. Spectral analysis

All the time series analyses discussed in this paper were performed using Analyseries (Paillard et al., 1996). Blackman–Tukey spectral analyses were performed using 3 different levels of confidence: 80%, 90% and 95%. Spectral peaks were filtered from the record using a wide range (frequency ± 20%) spectral band-pass filter, unless otherwise specified. Cross-spectral analyses to reveal spectral correlation and phase between the records were also performed using Analyseries, at the same 3 levels of confidence. A cross-correlation value over 90% is considered significant, a value over 95% is considered highly significant. Wavelet analysis was performed using the standard script of Torrence and Compo (1998), with a Morlet wave transform.

2.4. Ti/Al as a geochronological tool

The ratio of titanium to aluminum (Ti/Al) we have measured from the bulk sediment of ODP Sites 967 and 968 (Ziegler et al., 2010; Konijnendijk et al., 2014; this study) is interpreted as proxy for aeolian versus riverine-derived terrestrial materials transported to the studied sites, and as such inversely proportional to activity of the North African monsoon (Lourens et al., 2001). Windblown dust is estimated to be the source of 65%–95% of the titanium in the sediment (Wehausen and Brumsack, 2000; Lourens et al., 2001). The presence in the sediment of aluminum originates from clay minerals in the Nile outflow: a measure of runoff on the North African continent. Changes in Ti/Al mirror monsoonal-induced humidity changes in central to North Africa (Lourens et al., 2001), which is driven by changes in the earth's orbit, mainly precession (Rossignol-Strick, 1985). The most important reason to apply the Mediterranean Ti/Al record for tuning, instead of the CR or Ba/Al, is that it shows an almost linear response to insolation forcing also within 405-kyr eccentricity nodes when insolation changes are minor and sapropel depositions are lacking (Lourens et al., 2001; Konijnendijk et al., 2014).

2.5. Age model

ODP Site 967 is regarded as one of the most important reference sections for establishing the standard Pleistocene sapropel chronology of the Mediterranean (Emeis et al., 1996, 2000; Sakamoto et al., 1998; Kroon et al., 1998; Lourens 2004; Lourens et al., 1996). Following Lourens et al. (1996), the chronologies of the aforementioned authors were all based on the correlation of sapropel midpoints to their correlative 65°N summer insolation maxima, including a fixed 3-kyr time lag. Differences between them have occurred because of minor adaptations within the spliced record of ODP Site 967 and different correlation schemes. Here we follow the newest (refined) chronology of the combined ODP Site 967 and 968 record developed by Konijnendijk et al. (2014) for the past 1.05 Ma and extended their approach till 1.2 Ma.

For the upper 225 kyr of the record, Konijnendijk et al. (2014) use the ages of Ziegler et al. (2010), who dated this part in more detail than the initial standard sapropel chronology (e.g. Lourens et al., 1996, 2004) by correlating the color reflectance (CR) at 550 nm, Ba/Al and Ti/Al records of ODP Site 968 to the speleothem oxygen isotope ($\delta^{18}O_{speleothem}$) records of the Sanbao/Hulu caves (Wang et al., 2008). This correlation was based on the fact that the proxy records of both sites clearly reflect millennial-scale climate variability, which occurred superimposed on the dominant precession-controlled cyclicity associated with changes in the intensity of the monsoon system (Ziegler et al., 2010). In Konijnendijk et al. (2014), we followed this approach down to 340 ka, using the extended Chinese $\delta^{18}O_{speleothem}$ record of Cheng et al. (2009). Accordingly, the high precision U/Th dating of the Sanbao/Hulu caves (average dating error <1%; Cheng et al., 2009) could be transferred to ODP Sites 968 and 967, assuming an in-phase relationship between the millennial-scale variability observed in both records. Ziegler et al. (2010) relied primarily on correlating the CR record of ODP Site 968 to the Chinese $\delta^{18}O_{speleothem}$ record because the repeated depositions of at least 6 tephra layers and a thin turbidite slightly affected the Ti/Al signature over the past 225 ka. Below this point, the Ti/Al record no longer suffers from the occurrence of prominent tephra layers, and hence was used by Konijnendijk et al. (2014) and this study as primary tool for constructing the age model (Fig. 1). Note that we have removed 11 thin turbidites between 650 and 950 ka from our spliced record (Konijnendijk et al., 2014), based on their strong signature in the XRF record.

To establish the age model for the deeper part of our record we continued tuning the Ti/Al signal directly to the 65°N summer insolation target curve with a lag of ~2.7 kyr (Konijnendijk et al., 2014). The dating uncertainty in the speleothem record averages ~1.14 kyr (Cheng et al., 2009), and the standard deviation of the precession-related time lag is ±1.1 kyr. Root mean square error calculation of these values means there is a minimal uncertainty of ±1.6 kyr for all age estimates beyond ~340 ka, the last tie point between our record and the Chinese $\delta^{18}O_{speleothem}$ record. However, the smallest lag observed in the speleothem response is 0.8 kyr at ~105 ka (around sapropel S4), the largest is 3.7 kyr at ~240 ka (around S9). This means that the lag between insolation and the Ti/Al signal could conceivably vary by at least as much. To be on the

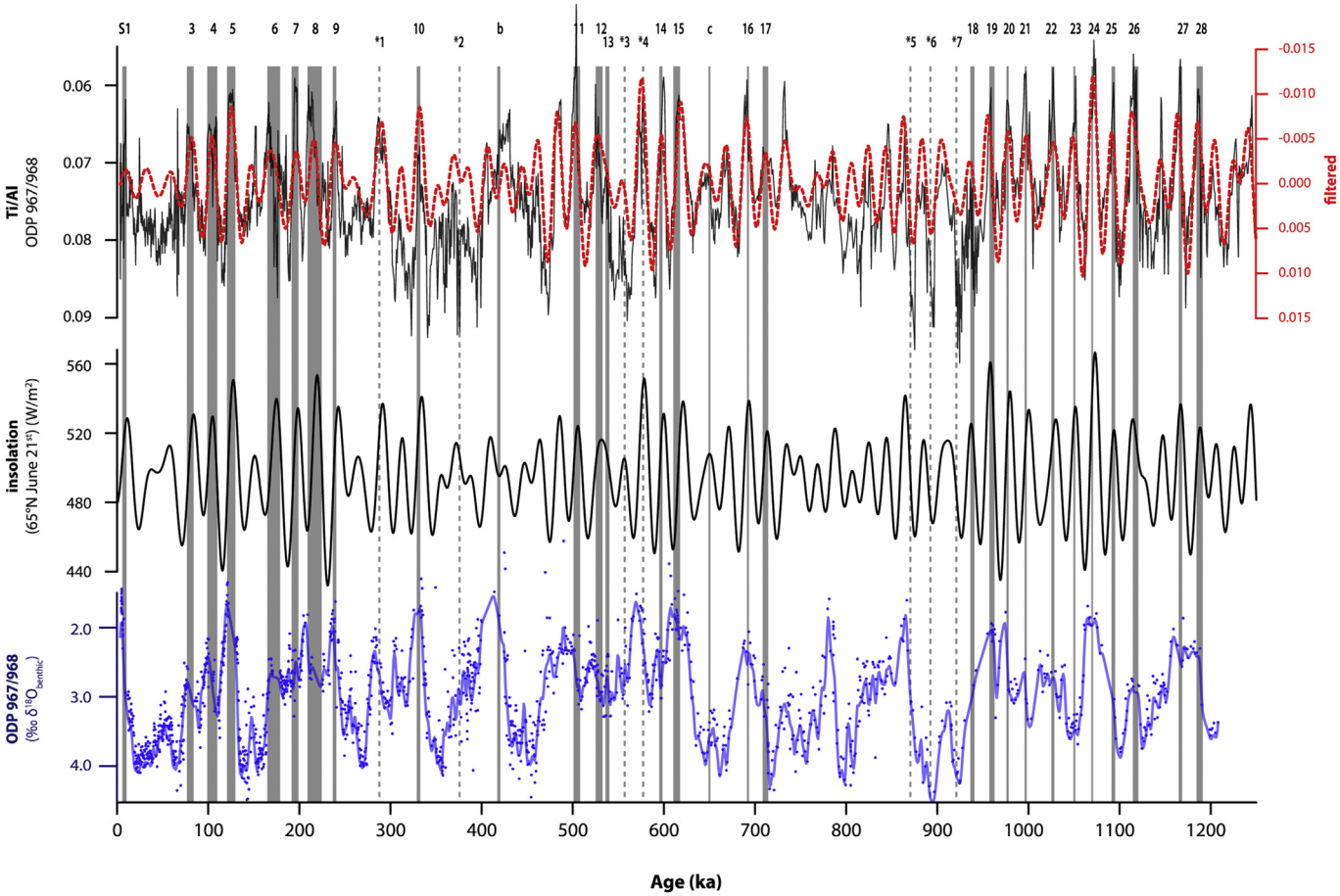

Fig. 1. Overview of the Ti/Al and benthic isotope data derived from the Eastern Mediterranean splice in relation to insolation (Laskar et al., 1993). The top graph in black is the Ti/Al proxy used for establishing the age model. The red overlay is a combination of the 23 kyr and 41 kyr signal recognized by a spectral filter (Paillard et al., 1996) after tuning, closely resembling the 65°N June 21st insolation curve (middle plot). The bottom graph is the benthic $\delta^{18}O$ record established from the Mediterranean splice. Individual measurements are indicated with blue dots. The gray line is a Gaussian low-pass (>5 kyr) filter to reduce noise. The vertical gray bars indicate sapropels as present in the Mediterranean splice (Konijnendijk et al., 2014). (For interpretation of the references to color in this figure legend, the reader is referred to the web version of this article.)

safe side, we assume that the precession-related time lag of the Ti/Al record may vary between 0 and 4 kyr. Results may correspondingly suffer from a 1.3 kyr overestimation or a 2.7 kyr underestimation of the age of individual cycles. Intervals with less pronounced eccentricity, in particular the 400 kyr minima at 400 ka (Marine Isotope Stage, or MIS, 11) and 800 ka (MIS 19) raise some additional uncertainty due to the weakly expressed cyclicity in the Ti/Al record. This will be discussed in Section 4.

With this overall robust and independent age model underlying our benthic isotope record, we compare the length and phase of the isotopic stages in the Pleistocene. We investigate the response of global climate and ice volume to insolation changes in view of the assumptions made by Imbrie and Imbrie (1980). We comment on the accuracy of existing chronologies like the LR04 benthic stack.

3. Results

3.1. Oxygen isotope record

All major glacial and interglacial stages (MIS1-35) of the past 1.2 Ma can be identified in the eastern Mediterranean benthic $\delta^{18}O$ record (Fig. 2). The transitions between stages are present without exception, making detailed estimation of the age and duration of all stages possible. The record shows some small gaps however, due to the occurrence of several episodes in which a number of successive samples are devoid of benthic foraminifers. In the last 250 kyr, these gaps in the record occur exclusively within the sapropel layers (Fig. 1), hinting at hydrographical changes, i.e. low-oxygen conditions in consequence of water column stratification, as the cause for their disappearance (Rossignol-Strick, 1985). Gaps in the record also occur below 250 ka, during MIS 9, 11, 17, 21, 25 and 27 (Fig. 1). Though often not accompanied by a fully developed sapropel, the interglacial setting may have triggered similar conditions too unfavorable for *G. neosoldanii* and *G. altiformis* to have lived at this site.

Isotopic values in the top ~0.9 Ma range from ~1.5‰ during interglacials to ~4‰ during full glacial conditions. Between 0.9 and 1.2 Ma the values range between 1.7 and 3.5‰. Late Pliocene values (MIS 96–100) reported for this core (Lourens et al., 2010) ranged from ~2‰ to ~3.1‰, respectively, meaning that the amplitude has increased during the Pleistocene, with a slight tendency toward heavier values. An increase in glacial/interglacial variability occurs around MIS 22 (900 ka), which has the heaviest isotope values measured in this record. It is a clear stepwise change towards full glacial values as found in the late Pleistocene.

In comparison to the LR04 benthic stack, the eastern Mediterranean record generally has much lighter isotopic values (Fig. 2) due to an on average higher water temperature than the global ocean (Ziegler et al., 2010). The difference ranges between 0.5 and 1.0‰ during glacial maxima and 1.0–1.5‰ during interglacial periods. The amplitude of glacial/interglacial variability is somewhat higher than the open ocean LR04 benthic stack due to the basin

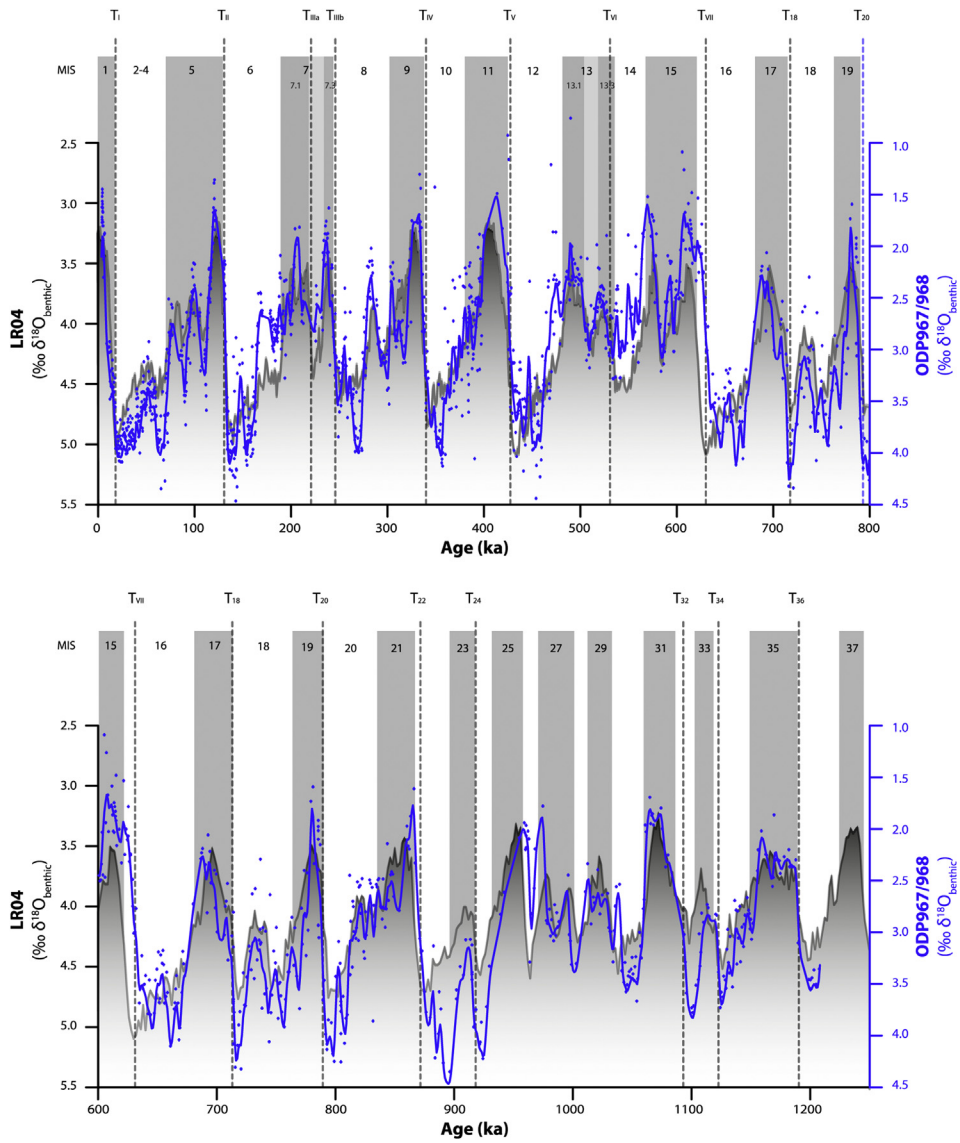

Fig. 2. Direct comparison of the Mediterranean benthic isotope record (blue dots and line) to the LR04 benthic stack (gray) (Lisiecki and Raymo, 2005). Marine isotope stages as published by Lisiecki and Raymo (2005) are indicated with gray (warm stages) and white (cold stages) background. Terminations as found in our study are indicated with vertical dashed lines. (For interpretation of the references to color in this figure legend, the reader is referred to the web version of this article.)

effect (Rohling, 1999). This effect is a result of the fact that the Mediterranean is a net evaporative basin with limited exchange to the open ocean. The restriction of water exchange with the open ocean through the Strait of Gibraltar causes significant regional hydrological effects as sea level changes over glacial/interglacial time (Rohling et al., 2014). Finally, the open ocean stack shows a more gradual increase in the full and mean glacial values over the course of the Pleistocene than the stepwise transition around MIS 22 in our record. Despite these differences, the two records exhibit a roughly identical signature on a glacial–interglacial scale.

3.2. Time series analysis

A wavelet conversion of the Mediterranean isotopes as well as the LR04 benthic stack indicates that the obliquity-related 41 kyr cycle and the well-known ~100-kyr glacial rhythm are the most persistent cycles in both records throughout the Pleistocene (Fig. 3). There are no indications for a distinct decrease in 41 kyr power from the early to the late Pleistocene, in association with the MPT. However, there are a couple of brief intervals, i.e. during MIS 13, 27, and 35, where the record does not show a clear 41 kyr signal (Fig. 3). Its absence during MIS 35 could be due to the fact that it occurs close to the edge of our record. MIS 13 and 27 are two intervals of low variability and with a higher frequency, ~29 kyr and 19 kyr respectively. A persistent influence of precession becomes visible in both records after ~400 ka and is clearly modulated by the 100-kyr cycle of eccentricity (Fig. 3).

Cross-spectral analysis between our record and the LR04 stack over the past 1.2 Ma reveals very similar power spectra (Fig. 4a). Both records reveal strong power around the 100 kyr period, secondary power in the 41 kyr obliquity-related frequency band, and to a lesser amount in the 23 kyr precession-related frequency band. A modest concentration of power is also found around 26.5 kyr in our Mediterranean record and around 29 kyr in LR04. Both records clearly lack power in the 19 kyr precession-related frequency band. Overall coherency is high, with values above the 95% significance level at 100 kyr, 41 kyr, 29 kyr and 23 kyr periodicities (Fig. 4b). There is a lesser but significant coherency peak at 19 kyr. The phase

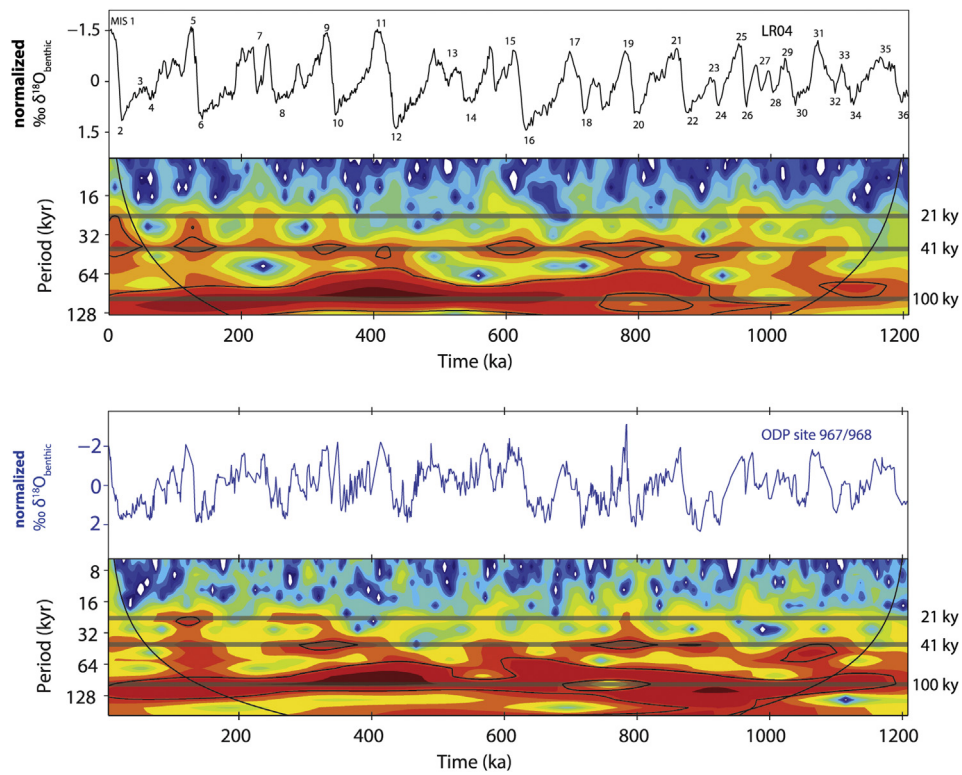

Fig. 3. (top) the normalized LR04 record, with a wavelet transform below. Horizontal bars indicate the standard Milankovic periodicities 100, 41, and 21 kyr. Compare the normalized Mediterranean benthic isotope record and its wavelet transform (bot).

spectrum shows that our record has a shorter lag for obliquity and a longer lag for precession than the LR04 stack (Fig. 4c). The difference amounts to −1.5 ± 0.4 kyr for obliquity and +1.3 ± 0.3 kyr for precession. Note that the uncertainty margins reported for phase estimates concern only the analytical uncertainty.

Subsequently, we applied cross-spectral analysis between our isotope record and the 65°N June 21st insolation (Fig. 4d–f). Coherency is high between both records in the precession and obliquity frequency bands with values exceeding the 95% significance level (Fig. 4). The analyzed phase relations over the past 1.2 Ma arrive at 5.5 ± 0.8 kyr for obliquity and 6.0 ± 1.0 kyr for precession.

The change in character of the $\delta^{18}O$ variability prior to MIS 22 suggests a change in relation to insolation. We performed a separate spectral analysis on the record 0–0.9 Ma and 0.9–1.2 Ma. Note that the 0.9–1.2 Ma is shorter and of lower resolution than the 0–0.9 Ma interval, which affects the reliability of the analysis. Results do indicate a faster response to obliquity forcing in the early Pleistocene than in the late Pleistocene (Fig. 5). The phase lags are estimated 3.0 ± 3.3 kyr for obliquity in the early Pleistocene, versus 5.7 ± 1.1 in the last 0.9 Ma. The analytical uncertainty of the >900 ka interval is relatively large due to the brevity of the interval. This result therefore awaits confirmation with the help of more and longer independently dated records. The results for precession are much closer together and fall well within the error margin, indicating little significant change.

3.3. Timing of glacial terminations

To identify the possible (orbital) forcing mechanism behind deglaciations in the Pleistocene, we followed Huybers and Wunsch (2004) and Huybers (2007, 2011), who analyzed the phase between the major glacial terminations and the main insolation variables obliquity and climatic precession (Fig. 6). First we determined the age of the terminations in our record, using the approach described by of Huybers (2007) and Grant et al. (2014). For this purpose we took the derivative of the benthic isotope record, which was first smoothed with a Gaussian filter, and identified the terminations as the interval where the sum of $\delta^{18}O$ change in a moving window of 4 kyr exceeds 0.8‰. This threshold is set to avoid smaller excursions and identify only the largest of deglaciation events. We average the onset and end of the termination interval to pinpoint an age (Fig. 6). The exact timing depends on the threshold used and the amount of smoothing but is not very sensitive: the estimates stay within our ±1.6 kyr uncertainty margin for a large range in threshold values. Local influences of hydrological changes (i.e. strong net evaporation) and temperature on our record will arguably have a larger influence on this measure. Nevertheless it provides us with a first order approach of the timing of glacial terminations as estimated using our Ti/Al age model (Table 1).

The age model for our record results in more or less identical estimates for the duration and timing of the boundaries for most of the marine isotope stages as described in LR04. There are, however, some mismatches beyond ~400 ka (Fig. 2). In first instance, the age for the onset of MIS 13.1 is estimated at 504.5 ± 1.6 ka in our record, which is ~3 kyr younger than the ~508 ka estimate in LR04. The age of the base of MIS 13.3 (i.e. T_{VI}) is ~6 kyr younger in our record (at ~526.5 ± 1.6 ka) than in LR04 (at ~533 ka). The age estimates of both records for the youngest interstadial in MIS 15 are in generally good agreement, though we estimate the onset of MIS 15 (T_{VII}) to be much older than in LR04: 630 ± 1.6 ka instead of 621 ka. Note that the latter is the age listed in Lisiecki and Raymo (2005), whereas our analysis of the LR04 stack indicates an age of ~624 ka. We found no large disagreements in the timing of MIS 17–23 (~650–900 ka) that transcend the uncertainty of our record. However, the onset of MIS 25 (T_{26}) is estimated ~3 kyr older, and MIS 27–6 kyr younger

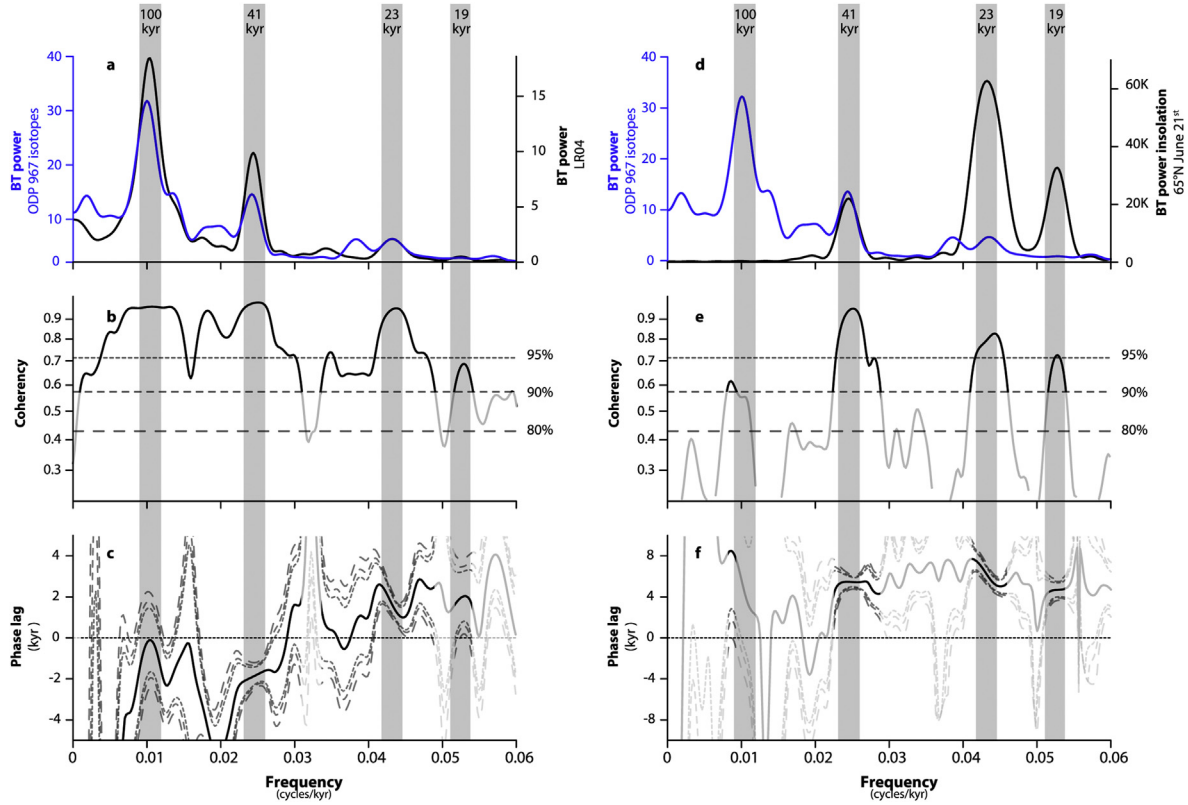

Fig. 4. a) in blue the Blackman–Tukey power spectrum of the Mediterranean benthic oxygen isotope record, and in black that of the LR04 benthic stack (Lisiecki and Raymo, 2005). The spectra look very similar with a dominant spectral peak at 100 kyr, secondary power at 41 kyr and a smaller peak at 23 kyr b) coherency between the Mediterranean isotope record and LR04. Horizontal dashed lines indicate confidence levels. Coherency is consistently high (>95%) in all periods higher than 33 kyr as well as around 23 kyr. Significant (>90%) coherence also occurs at 29 kyr (0.034 cycles/kyr). c) Phase difference between the Mediterranean isotope record and insolation, in kyr. The high coherency translates into a narrow uncertainty envelope (dashed lines) at the dominant spectral frequencies. d–f) the same for the cross correlation between the Mediterranean benthic isotope record and June 21st insolation at 65°N. For all frequencies where coherency is below the 90% significance level, coherency and phase values are plotted semi-transparent. (For interpretation of the references to color in this figure legend, the reader is referred to the web version of this article.)

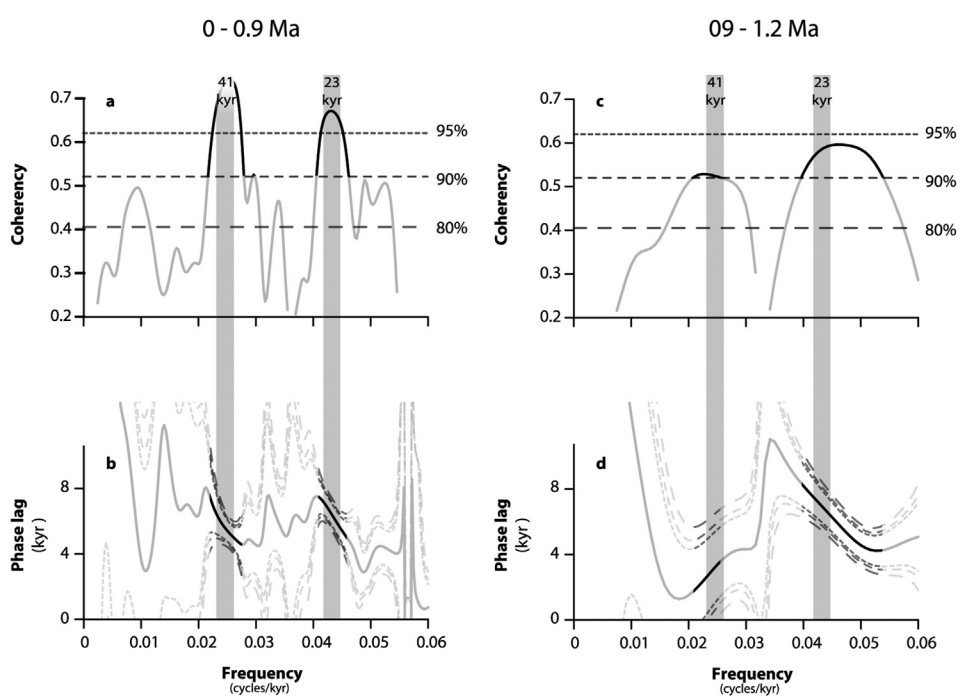

Fig. 5. a–b) coherency and phase between the isotope record and insolation over the last 900 ka (as in Fig. 4). c–d) the same for the interval 900–1200 ka. The shorter interval and low resolution translate to higher uncertainties, though they remain significant. The lag to obliquity is considerably shorter in the early Pleistocene, but for precession there is little change.

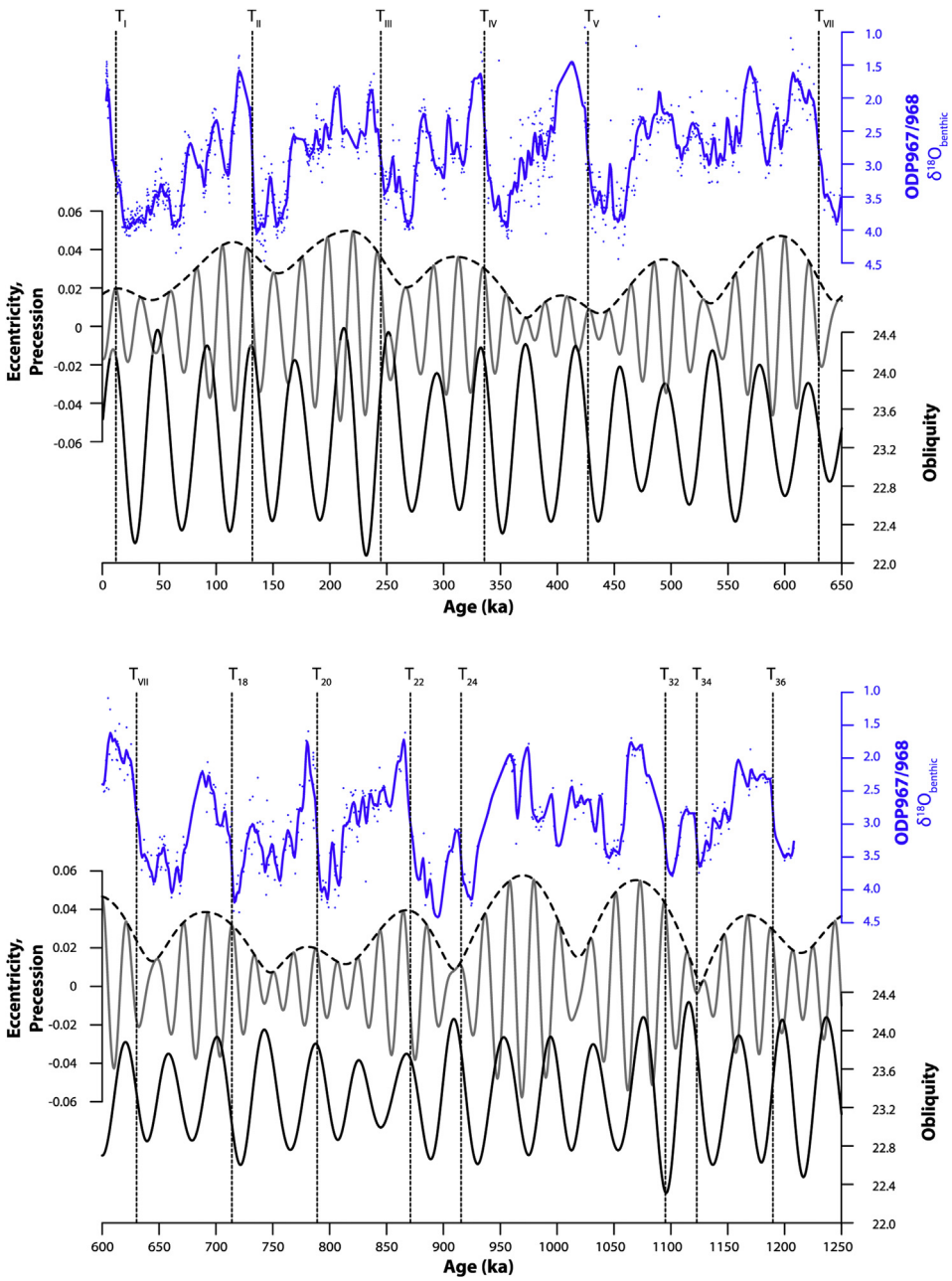

Fig. 6. Direct comparison of the Mediterranean benthic isotope record (blue dots and lines, as in Fig. 1) to the orbital parameters obliquity (bottom graph in both plots), eccentricity, and climatic precession (middle graphs). Terminations are indicated by vertical dashed lines. (For interpretation of the references to color in this figure legend, the reader is referred to the web version of this article.)

than in LR04 (Fig. 2). This gives our record a very different character in relation to insolation during this interval, even though the variability is similar to that in the open ocean stack. Our estimate for stages 28–32 agrees well with the LR04 stack again, although we note a short-lived excursion in MIS 30 that is not reflected in LR04. The age of the base of MIS 35 (T_{36}) is again in very good agreement with LR04, while the onset of MIS 33 (T_{34}), having a slightly different shape, is ~3 kyr older.

In a next step, we compared the timing of the terminations with the astronomical parameters of precession and obliquity by estimating the phase lag between each termination and the closest onset of a precession or obliquity cycle (defined as the maximum rate of change). The results are portrayed in a phase wheel (Fig. 7), where the angle indicates the phase lag relative to each variable. Considering the uncertainty in our age model (see §2.5), we refrain from making detailed statements on details regarding the exact timing of the terminations. We only consider the cases where we can exclude deglaciation events to be related to either precession or obliquity. We exclude de possibility of either parameter when the timing of a deglaciation deviates more than 1σ from the average. This comes down to a lag of more than 12.5 kyr to obliquity, or a lead of 1.9 kyr. For precession, a lag of more than 5.7 kyr or a lead of more than 1.1 is considered impossible. Note that all the deglaciation events included in our discussion would fall outside this range, even if our tuning lag is overestimated by the full 2.7 ± 1.6 kyr, or underestimated by the full 1.3 ± 1.6 kyr, by which the Ti/Al tuning could conceivably vary. Terminations T_{IIIa} (missing) and T_{VI} (unreliable) are omitted, because the nature of these deglaciations makes

Table 1
The timing of terminations in ka. Terminations T_I–T_{VII} are identified as defined by Raymo (1997), T_{18}–T_{36} follow the unofficial protocol of Lourens et al. (2010) and are named after the glacial MIS that they end. The timing is determined as explained in §3.3, for both the Mediterranean isotope record (second column) and LR04 (third column). The ages of T_I–T_{VII} as listed in Lisiecki and Raymo (2005) are added (fourth column) for reference.

Deglaciation	This study	LR04 *(this study)*	LR04 *(listed)*
T_I	17.3	16	14
T_{II}	134.4	134	130
T_{III}	244.4	244	243
T_{IV}	338.4	336	337
T_V	427.1	429	424
T_{VI}		534	533
T_{VII}	629.1	624	621
T_{18}	715.6	715	
T_{20}	791.3	793	
T_{22}	870	867	
T_{24}	916.4	917	
T_{26}		961	
T_{28}		1001	
T_{30}		1032	
T_{32}	1095.8	1096	
T_{34}	1123.7	1121	
T_{36}	1190.7	1189	

them unsuitable for our analysis. In addition, the isotope shift at the onset of MIS 13.3 is too small and too slow to pass the threshold in our approach.

The timing of T_{IIIb} and of T_{36} lag obliquity by more than 140° or 16 kyr. Termination T_{32} on the other hand leads obliquity by >70° or 8 kyr. However, an exact determination of the timing of T_{32} is problematic in the Mediterranean record, due to a gap in the isotope record in the later part of the termination. This might influence our analysis. T_{18} leads obliquity by 18° or 2.1 kyr. Each of these terminations have a quite realistic lag – between 30° and 70°, or ~2–4 kyr – relative to precession. We consider these terminations as the result of precession forcing only, and reject the possibility of obliquity as a driver. The attribution of terminations T_{36} (and potentially T_{32}) to precession supports an early onset of the MPT. On the other hand, T_{VII} and T_{34} lead precession (>60°, more than ~4 kyr), while they all have a normal (if small) lag to obliquity (between 0° and 30°, or ~0–3 kyr). We must reject precession as a driver of T_{VII}, which is remarkable because it is considered to mark the beginning of the 'full 100 kyr world' at the end of the MPT (Clark et al., 2006).

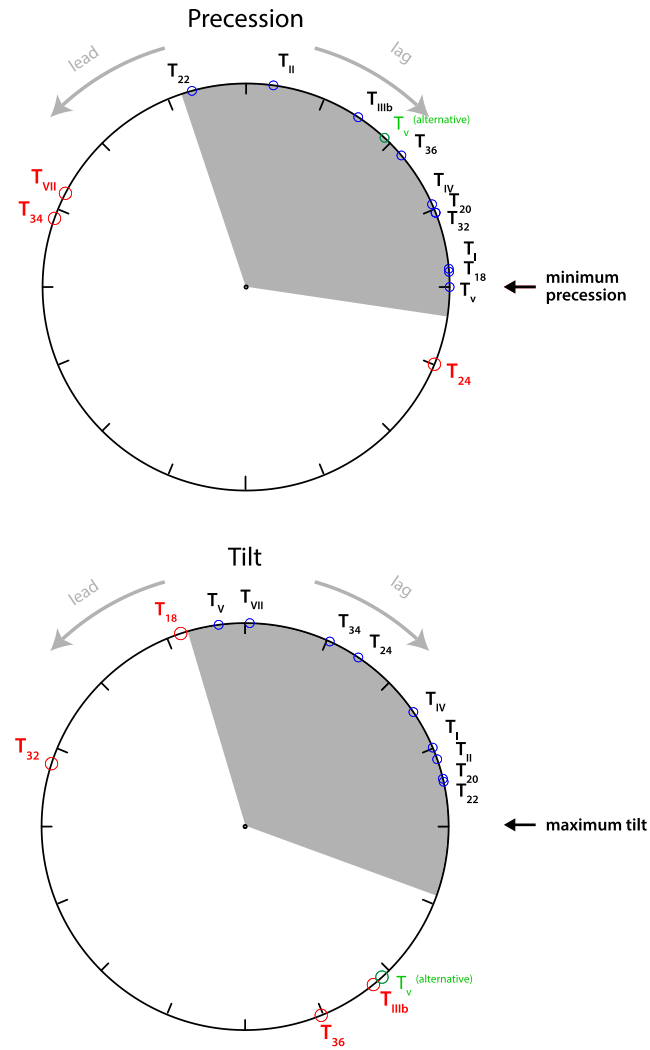

Fig. 7. Phase wheel showing the phase estimate of the terminations as indicated in Fig. 6 with respect to the nearest onset in the cycles of obliquity (left) and precession (right). Zero degrees means no lag, 90° corresponds to a ¼λ, or ~10 kyr (obliquity), ~5 kyr (precession). Termination T_{III} (~245 ka) means $T_{III\text{-}b}$: Termination $T_{III\text{-}a}$ is not indicated because it is missing from our record. The shaded area in the graphs is the 1σ range of terminations. Terminations that fall outside this range are marked in red to indicate that they are unlikely to be triggered by this insolation variable. (For interpretation of the references to color in this figure legend, the reader is referred to the web version of this article.)

4. Discussion

The overall level of agreement between our Mediterranean record and the LR04 stack is high (Fig. 2). Nevertheless, we observed a number of features in our record that are different from the open ocean stack (see §4.2). Because our record is situated within the semi-enclosed basin of the Mediterranean, these features most likely arise from regional changes in temperature and hydrology. Overall however, our record primarily follows changes in global ice volume, with similar changes in deep sea temperature similar to those found in the open ocean. This observation is underlined by the fact that our Mediterranean benthic $\delta^{18}O$ record reveals comparable ages for most of the glacial–interglacial transitions and isotopic stages to those in LR04 (Table 1). The exceptions to this rule are (the interstadials of) MIS 13, 15, 25, 27, and 33, which deviate considerably. In addition, we found several characteristic isotopic features in our Mediterranean benthic $\delta^{18}O$ record which were not reflected in the open ocean benthic stack LR04 (Fig. 2), namely: (1) The larger amplitude of our record with respect to the open ocean (2) Our record exhibits short-lived negative excursions immediately preceding glacial terminations. (3) some glacial inceptions appear to have a different structure, e.g. MIS 6 and 12. (4) The isotope values in our record curve more smoothly into glacial terminations, in contrast to the jagged sawtooth shapes of the LR04 stack. We can largely exclude inter-laboratory discrepancies as possible explanation for these differences, because the accuracy and analytical precision of the oxygen isotope measurements are in general high. The few gaps in our isotope record of the interval encompassing MIS 25–27 and several sapropel layers were excluded from our discussion and hence cannot explain the observed differences either. On the contrary, the largest differences we recognized occurred in the intervals which have good data coverage (Fig. 2). This implies that the aberrant features reflected in the Mediterranean benthic $\delta^{18}O$ record are most likely due to uncertainties between the two chronological approaches and the possible imprint of regional temperature and hydrological effects.

4.1. Accuracy of the Ti/Al time scale

Our confidence in the Ti/Al-based age model is high, since the dominant precession cyclicity is readily apparent from spectral analysis of the untreated record in the depth domain (Konijnendijk et al., 2014). After tuning (to precession only), the spectral power carries great resemblance to overall insolation (Fig. 1), confirming the highly linear response of Ti/Al to the forcing. A possible source of uncertainty may however come from the constant time lag of 2.7 kyr we applied between the Ti/Al record and insolation. In comparison, the Chinese $\delta^{18}O_{speleothem}$ response to insolation has a lag varying between 0.8 ± 0.4 kyr and 3.6 ± 1.6 kyr. The largest deviations from the mean lag occur during the eccentricity minima, when the precession-bound signals are weak. The deviations are not systematic, i.e. no recurring faster or slower response during forcing minima, as far as our analysis can find. Therefore we have kept our tuning lag constant.

An interval with increased uncertainty is the period of weakly expressed precession around T_V, which also contains sapropel S_b (Fig. 1). According to the Ti/Al age model (Konijnendijk et al., 2014) this sapropel one i-cycle older than previous studies (Emeis et al., 2000; Lourens, 2004). In this interval, the 41 kyr band pass filter we applied to our benthic oxygen isotope record follows the obliquity component of insolation well, though there are some inconsistencies during MIS 12 and 13. Here the amplitude of the filtered signal is much smaller than in the adjacent cycles, whereas this change is not reflected in the obliquity forcing (Fig. 8). Also, the lag of the 41 kyr component to insolation is decreased in MIS 9 and 10, to an almost in-phase state. After MIS 9 the 41 kyr component continuously lags insolation again.

To test the validity of our age model, we re-tuned the Ti/Al record to insolation in the interval ~350–560 ka, adjusting tie points so that sapropel S_b has an age of ~407 ka, in accordance with the adopted age of Lourens (2004). The corresponding ages for the isotopic record also shifted (Sup. Fig. 1), which improved the results of the 41 kyr spectral band filter (Sup. Fig. 2): a more consistent phase behavior and no more amplitudinal irregularities. The resulting phase lag estimates for the isotopic record are ~6.8 kyr for obliquity and ~6.7 kyr for precession. What is more important, however, is that attributing S_b to a later i-cycle also shifts T_v, which occurs at about the same depth, to 411.3 ka. This contradicts both the LR04 and EDC chronologies for this termination, but agrees with Shackleton (1995), who also placed T_v at ~410 ka.

A major consequence of this alternative tuning is the radical change in sedimentation rate at the MIS 12-MIS 11 transition (Sup. Fig. 3). Also, a ~15 kyr mismatch in the LR04 benthic stack would indicate a pronounced perturbation of the global mean sedimentation rate, which is a powerful argument against such a revision in this well resolved interval of the stack (Lisiecki and Raymo, 2005). Finally, while the spectral filter for the isotopic record was improved, the spectral filters for the Ti/Al record were negatively affected by the change in tuning (Sup. Fig. 3a, b), illustrating that the alternative tuning does not match insolation forcing as well as in the original tuning (Konijnendijk et al., 2014).

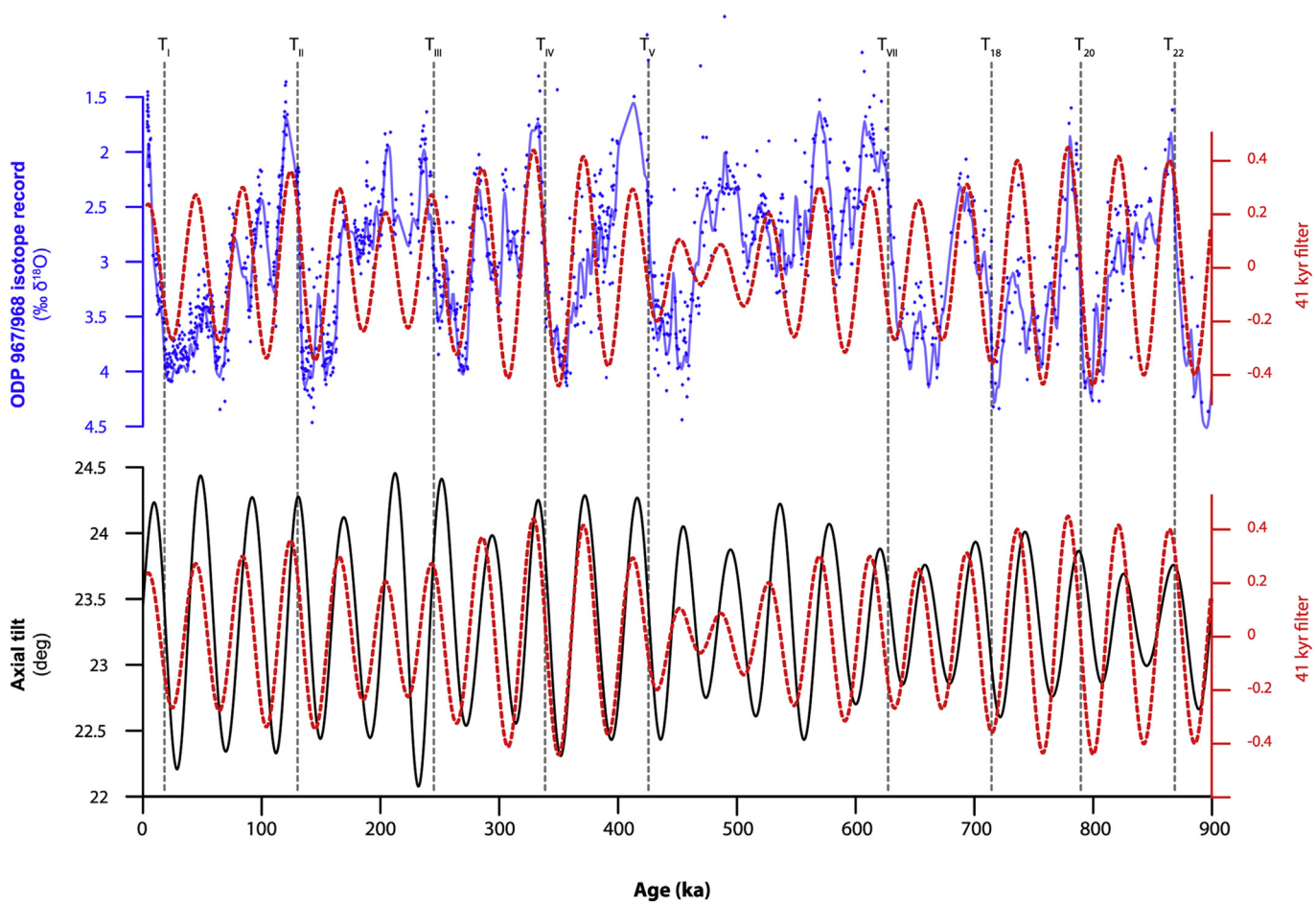

Fig. 8. a spectral band pass filter centered on 41 kyr (frequency 0.0241 ± 0.005; dashed red line) versus the Mediterranean isotope record (blue dots and line) and versus obliquity (black line). (For interpretation of the references to color in this figure legend, the reader is referred to the web version of this article.)

4.2. Regional temperature and hydrological effects

The larger glacial–interglacial amplitude of the Mediterranean benthic $\delta^{18}O$ record most likely implies a direct influence of regional temperature and hydrological changes in the semi-enclosed Mediterranean basin over glacial–interglacial time scales (Rohling, 1999; Rohling et al., 2014). Precession-controlled perturbations in the regional temperature and hydrological conditions of the Mediterranean basin, seem to have shaped the benthic $\delta^{18}O$ record as well. Most clearly are the precession-related short-lived excursions depicted in the record during MIS 6, 8, 12, and 14, that are neither as pronounced nor reflected in the open ocean benthic stack LR04 (Fig. 2). These small excursions just prior to deglaciations are in contrast to the LR04 stack also found in the sea level reconstructions of the Red Sea over the past 500 ka (Siddall et al., 2003; Rohling et al., 2009; Grant et al., 2012, 2014). This suggests that a regional hydrological effect is in play in both basins, thus possibly connected to changes in the low-latitude climates such as the monsoon. However, because similar features were also found in the Antarctic Epica Dome C ice core δDeuterium (δD_{ice}) record (Rohling et al., 2009), it seems more likely that these excursions are linked to and hence reflect global sea level changes (Rohling et al., 2014), which are evidently not resolved by the LR04 record.

Another marked difference are the shouldered slopes (i.e. early return to interglacial values) found at the onset of the deglaciations of MIS 10, 12, 16, and 22 in our record that seem to coincide with the most severe glacial values in LR04 (Fig. 2). These features generally occur in phase with or just before an increase in Northern Hemisphere summer insolation. We hypothesize that during these periods of relatively low insolation and extreme cold conditions in the North Atlantic region, the overall evaporation in the Mediterranean basin is low, thereby reducing the hydrological influence (i.e. less ^{16}O export) and hence concomitant $\delta^{18}O$ values of the eastern Mediterranean deep water that flows along these drill sites (Robinson et al., 1992).

To summarize, regional and/or local temperature or hydrological changes in the Mediterranean can explain the observed differences in shape and expression of the short-lived isotopic features between our record and LR04, noting that in particular the precession-related excursions were also found in records outside the Mediterranean realm. As a result, the Mediterranean $\delta^{18}O$ record has gained a less asymmetric saw tooth appearance through the late Pleistocene glacial cycles than LR04. This increased (pseudo) symmetry may have affected the average phasing of the orbital band pass filters and hence could explain the observed smaller time lag than assumed by LR04. Most of the glacial–interglacial transitions however are, due to the magnitude of the isotopic shift, so distinct that the offset due to regional and local effects in terms of timing of the terminations ought to be negligible compared to the actual discrepancies found between the records. Another source of uncertainty may stem from the LR04 chronology.

4.3. Chronological uncertainties in late Pleistocene records

Incongruences in age between the EDC δD_{ice} record and the LR04 benthic isotope stack were discussed by Parrenin et al. (2007) for their EDC3 time scale. In particular, the clear offset of +6 kyr they found between both chronologies for MIS 13. The EDC3 time scale is based on a detailed ice accumulation and flow model in combination with tuning of $\delta^{18}O$ from atmospheric O_2 in ice bubbles to insolation. The recently published Antarctic Ice Core Chronology 2012 (AICC2012) however changes the onset of MIS 13 considerably (Bazin et al., 2013). Bazin et al. (2013) omitted a tuning marker at ~532 ka, arguing it caused fluctuations in their ice accumulation model. This results in the deuterium record lining up with LR04 to an age estimate of 533 ka for the onset of MIS 13. Even with the large uncertainty range involved with the estimates (±6 kyr for EDC – Dreyfus et al., 2007; Bazin et al., 2013), the synchronicity between the AICC2012 chronology and the LR04 stack suggests our estimate to be incorrect. It could be that the Ti/Al age model is less accurate because of a lack of tie points due to the broad insolation maximum around 530 ka. Considering the double sapropels in this same interval (Fig. 1), it is also likely that local influences on our benthic isotope record disturb the estimate.

Apart from MIS 13, Parrenin et al. (2007) discussed the timing of termination T_{VII}, which leads LR04 by ~3 kyr. There is little change in the timing of this deglaciation in the AICC2012 chronology, at ~629 ka (Bazin et al., 2013). This estimate agrees with our age estimate of termination T_{VII} at 630 ± 1.6 ka (Fig. 9). The listed LR04 estimate (621 ka) is well outside the possible age range of the Ti/Al chronology.

Beyond T_{VII}, the lowest part of the EPICA Dome C record, there are more discrepancies between LR04 and the deuterium data, ranging from −2 kyr to +8 kyr. In this interval, our record is more closely aligned with LR04, disagreeing with the AICC2012 chronology (Fig. 9). This suggests that, whatever caused the later exceptions, for the period of ~650–900 ka the LR04 tuning is consistent with our Ti/Al based age model. This suggests that the AICC2012 chronology is marginally flawed in the lowermost part of the record.

Until now we have tacitly assumed that changes in benthic $\delta^{18}O$ occur more or less simultaneously in different basins throughout the Pleistocene. Recent work (Skinner and Shackleton, 2005; Lisiecki and Raymo, 2009) has shown, however, that there is a significant mismatch between the Pacific and the Atlantic basin, with T_I–T_V in the Pacific lagging the Atlantic by an average of ~1600 yrs (Lisiecki and Raymo, 2009). Unfortunately, there is no measure for any possible lag between the Mediterranean and the Atlantic because no benthic oxygen isotope record of sufficient length and resolution was available. We note here that, for T_I–T_V, we found no significant mismatch between our benthic record and

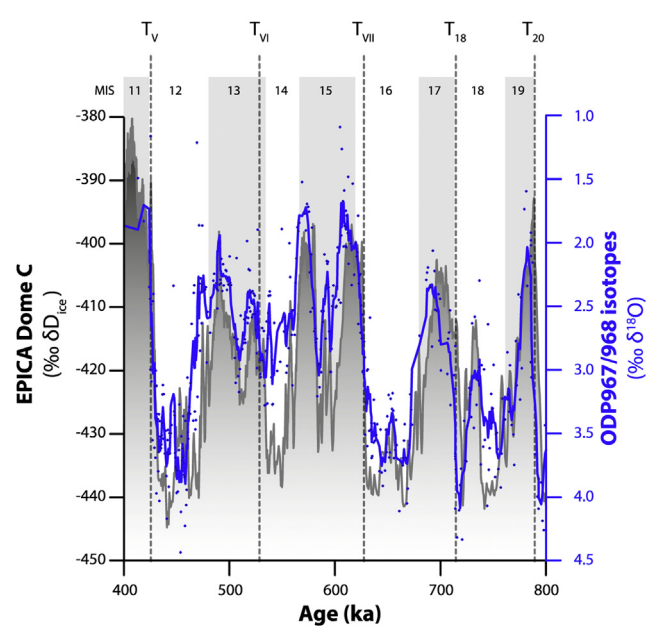

Fig. 9. Direct comparison of the Mediterranean benthic isotope record (blue dots and line) to the EDC δD_{ice} (Jouzel et al., 2007; Bazin et al., 2013), for MIS 11–19. As in Fig. 2. (For interpretation of the references to color in this figure legend, the reader is referred to the web version of this article.)

the average (Atlantic and Pacific) ages published for the LR04 benthic stack. In addition, our record leads LR04 in some stages, but significantly lags the benthic stack at other intervals. There does not seem to be a systematic deviation of Mediterranean benthic isotopes with regard to the average of the LR04 benthic stack. Our age model therefore provides an alternative to the one published by Lisiecki and Raymo (2005). We have re-tuned the LR04 stack accordingly and have made it available in the Supplementary material.

4.4. Phase of ice volume changes and glacial terminations

The disagreements between our record and the LR04 age model imply that the response of global ice volume and climate to insolation forcing is not as systematic as assumed by the Imbrie and Imbrie (1980) model. This may in part be due to the changes in the climate system responsible for the MPT. The shifting response of ice sheets, and with them global climate, from the obliquity to the precession parameter is difficult to capture in one tuning model.

Using phase estimates (Fig. 7) we have tried to identify which orbital parameter is likely to have caused each glacial–interglacial transition in the past ~1.2 Ma. Based on this analysis we exclude obliquity as a possible forcing for the onset of MIS 7, 17, 31, and 35. The exclusive role of precession forcing inferred for MIS 35 puts the onset of the MPT not later than ~1.2 Ma, consistent with the findings of Clark et al. (2006) and Dupont et al. (2001). The obliquity parameter remains important throughout the Pleistocene, as is clear by the timing of T_{VII}, and T_{34}. For T_{VII}, which is at the end of the MPT where the 100 kyr cycle is commonly regarded to be well established (e.g. Mudelsee and Stattegger, 1997; Clark et al., 2006), precession is unlikely to have influenced the timing of the deglaciation. The isotope shift occurs ~9 kyr earlier than estimated by LR04 and other authors (e.g. Shackleton, 1995; Huybers and Wunsch, 2004) but not the AICC2012 (Bazin et al., 2013), which times the transition at ~628 ka. That is within our uncertainty estimate. Such an early transition cannot be the result of precession forcing because it leads the nearest precession cycle by 62°, or ~3.6 kyr (Fig. 7). A combination of the parameters (Huybers, 2011) is also not likely, because the maximum rate of change in 65°N June 21st insolation – combining both precession and obliquity – occurs at or around the same time as the shift in precession, which would result in a similar phase relation. Our findings therefore suggest that this transition is forced solely by obliquity.

The phase wheel in Fig. 7 does not unambiguously show a difference in response time of global climate to insolation between the middle and the late Pleistocene. We therefore look to the cross-spectral analyses performed on the intervals in the record before and after ~0.9 Ma. These provide a more general estimate for the interval, instead of snapshots of individual transitions. We place the boundary here because it is the clearest single long term shift in climatic behavior (Mudelsee and Schulz, 1997; Elderfield et al., 2012; this study). The cross-spectral analyses over the intervals before and after 0.9 Ma show the phase lag of the isotope response to obliquity was likely to be considerably (~2.7 kyr) shorter in the early Pleistocene than in the last 900 ka (Fig. 5), although this result needs confirmation from more and longer independently dated records. These estimates stray significantly from those inferred (by e.g. Lisiecki and Raymo, 2005) from the model of Imbrie and Imbrie (1980), suggesting a much less systematic response than assumed in literature. Also, we have assumed that the lag in Ti/Al remains constant at 2.7 kyr throughout the record. It is likely that this lag would have been smaller in the early Pleistocene (Ziegler et al., 2010), causing an even larger difference in the inferred MIS ages.

5. Conclusions

We present the first long, high-resolution benthic isotope record from the eastern Mediterranean Sea. It reflects all the glacial and interglacial stages and interactions of the last ~1200 kyr present in the LR04 benthic stack. Using sediment geochemistry to create our age model we establish independent age estimates for the timing and duration of the Marine Isotopic Stages of the Pleistocene. We arrive at different ages for some isotopic stages compared to the LR04 benthic stack before MIS 11. (An updated age model for the LR04 benthic stack is provided in the Supplementary material.) We attempt to use our additional age control to pinpoint the influence of the orbital parameters obliquity and precession in triggering deglaciations. Though large uncertainties are involved, evidence indicates that terminations T_{32} and T_{36} are attributable to precession. This argues for an early (>1200 ka) onset of the MPT. Vice versa, the ~9 kyr earlier onset of T_{VII} compared to LR04 can only be explained as a response to obliquity forcing.

Spectral cross-correlation analysis of the record reveals significant amounts of power in the obliquity and precession range, with an average lag of 5.5 ± 0.8 kyr for obliquity, and 6.0 ± 1.0 kyr for precession. Separate analysis of the intervals before and after ~900 ka however reveal a lag of 3.0 ± 3.3 kyr to obliquity in the early Pleistocene, and a lag of 5.7 ± 1.1 kyr in the late Pleistocene. Our findings suggest that Earth's climate behaves less systematic with regard to insolation forcing than predicted by the deterministic approaches of Imbrie et al. (1984), Shackleton (1995), and Lisiecki and Raymo (2005).

Acknowledgments

This project was financially supported by NWO-ALW (project number 865.10.001). We kindly acknowledge the Ocean Drilling Program in general, and Walter Hale and the Bremen Core Repository specifically for the samples used in this study. Special thanks go to Astrid Vrijhoef for her assistance in lab work, and to Karlijn Groenewegen for valuable comments on methods. Several anonymous reviewers provided extensive feedback, helping to improve the manuscript considerably. This work was initiated by L.J. Lourens. Lab work and analyses were performed by M. Ziegler and T.Y.M. Konijnendijk. T.Y.M. Konijnendijk wrote the manuscript, with contributions of the other authors.

Appendix A. Supplementary data

Supplementary data related to this article can be found at http://dx.doi.org/10.1016/j.quascirev.2015.10.005.

References

Bard, E., Hamelin, B., Fairbanks, R.G., 1990. U-Th ages obtained by mass spectrometry in corals from Barbados: sea level during the past 130,000 years. Nature 346, 456–458.

Bazin, L., Landais, A., Lemieux-Dudon, B., Toyé Mahamadou Kele, H., Veres, D., Parrenin, F., Martinerie, P., Ritz, C., Capron, E., Lipenkov, V., 2013. An optimized multi-proxy, multi-site Antarctic ice and gas orbital chronology (AICC2012): 120–800 ka. Clim. Past 9, 1715–1731.

Bintanja, R., van de Wal, Roderik SW., Oerlemans, J., 2005. Modelled atmospheric temperatures and global sea levels over the past million years. Nature 437, 125–128.

Cheng, H., Edwards, R.L., Broecker, W.S., Denton, G.H., Kong, X., Wang, Y., Zhang, R., Wang, X., 2009. Ice age terminations. Science 326, 248–252.

Clark, P.U., Archer, D., Pollard, D., Blum, J.D., Rial, J.A., Brovkin, V., Mix, A.C., Pisias, N.G., Roy, M., 2006. The middle Pleistocene transition: characteristics. Mechanisms, and implications for long-term changes in atmospheric PCO2. Quat. Sci. Rev. 25, 3150–3184.

Dreyfus, G., Parrenin, F., Lemieux-Dudon, B., Durand, G., Masson-Delmotte, V., Jouzel, J., Barnola, J., Panno, L., Spahni, R., Tisserand, A., 2007. Anomalous flow below 2700 m in the EPICA dome C ice core detected using $\delta^{18}O$ of atmospheric

oxygen measurements. Clim. Past 3, 341–353.
Dupont, L., Donner, B., Schneider, R., Wefer, G., 2001. Mid-Pleistocene environmental change in tropical Africa began as early as 1.05 ma. Geology 29, 195–198.
Dutton, A., Bard, E., Antonioli, F., Esat, T.M., Lambeck, K., McCulloch, M.T., 2009. Phasing and amplitude of sea-level and climate change during the penultimate interglacial. Nat. Geosci. 2, 355–359.
Elderfield, H., Ferretti, P., Greaves, M., Crowhurst, S., McCave, I.N., Hodell, D., Piotrowski, A.M., 2012. Evolution of ocean temperature and ice volume through the Mid-Pleistocene climate transition. Science (New York, N.Y.) 337, 704–709.
Emeis, K.C., Robertson, A., Richter, C., 1996. Proceedings of the Ocean Drilling Program, Initial Reports, vol. 160. ODP, College Station (TX).
Emeis, K., Sakamoto, T., Wehausen, R., Brumsack, H.J., 2000. The sapropel record of the eastern Mediterranean Sea — results of Ocean Drilling Program Leg 160. Palaeogeogr. Palaeoclimatol. Palaeoecol. 158, 371–395.
Gradstein, F.M., Ogg, J.G., Smith, A.G., Bleeker, W., Lourens, L.J., 2004. A new geologic time scale, with special reference to Precambrian and Neogene. Episodes 27, 83–100.
Grant, K., Rohling, E., Bar-Matthews, M., Ayalon, A., Medina-Elizalde, M., Ramsey, C.B., Satow, C., Roberts, A., 2012. Rapid coupling between ice volume and polar temperature over the past 150,000 [thinsp] years. Nature 491, 744–747.
Grant, K., Rohling, E., Ramsey, C.B., Cheng, H., Edwards, R., Florindo, F., Heslop, D., Marra, F., Roberts, A., Tamisiea, M., 2014. Sea-level variability over five glacial cycles. Nat. Commun. 5.
Grossman, E.L., 1984. Stable isotope fractionation in live benthic foraminifera from the Southern California Borderland. Palaeogeogr. Palaeoclimatol. Palaeoecol. 47, 301–327.
Harmon, R.S., Schwarcz, H.P., Ford, D.C., 1978. Late Pleistocene sea level history of Bermuda. Quat. Res. 9, 205–218.
Harmon, R.S., Mitterer, R.M., Kriausakul, N., Land, L.S., Schwarcz, H.P., Garrett, P., Larson, G.J., Vacher, L., Rowe, M., 1983. U-series and amino-acid racemization geochronology of Bermuda: implications for eustatic sea-level fluctuation over the past 250,000 years. Palaeogeography. Palaeogeogr. Palaeoclimatol. Palaeoecol 44 (1), 41–70.
Hays, J.D., Imbrie, J., Shackleton, N.J., 1976. Variations in the Earth's orbit: Pacemaker of the ice ages. Science 194 (4270), 1121–1132.
Huybers, P., Wunsch, C., 2004. A depth-derived Pleistocene age model: uncertainty estimates, sedimentation variability, and nonlinear climate change. Paleoceanography 19, PA1028.
Huybers, P., 2011. Combined obliquity and precession pacing of late Pleistocene deglaciations. Nature 480, 229–232.
Huybers, P., 2007. Glacial variability over the last two million years: an extended depth-derived agemodel, continuous obliquity pacing, and the Pleistocene progression. Quat. Sci. Rev. 26, 37–55.
Imbrie, J., Berger, A., Boyle, E.A., Clemens, S.C., Duffy, A., Howard, W.R., Kukla, G., Kutzbach, J., Martinson, D.G., McIntyre, A., et al., 1993. On the structure and origin of major glaciation cycles 2. the 100,000-year cycle. Paleoceanography 8, 699–735.
Imbrie, J., Hays, J.D., Martinson, D.G., McIntyre, A., Mix, A.C., Morley, J.J., Pisias, N.G., Prell, W.L., Shackleton, N.J., 1984. The orbital theory of Pleistocene climate: support from a revised chronology of the marine $\delta^{18}O$ record. In: Milankovitch and Climate. Understanding the Response to Astronomical Forcing, vol. 1, p. 269.
Imbrie, J., Imbrie, J.Z., 1980. Modeling the climatic response to orbital variations. Science (New York, N.Y.) 207, 943–953.
Jouzel, J., Masson-Delmotte, V., Cattani, O., Dreyfus, G., Falourd, S., Hoffmann, G., Minster, B., Nouet, J., Barnola, J.M., Chappellaz, J., et al., 2007. Orbital and millennial Antarctic climate variability over the past 800,000 years. Science (New York, N.Y.) 317, 793–796.
Konijnendijk, T., Ziegler, M., Lourens, L., 2014. Chronological constraints on Pleistocene sapropel depositions from high-resolution geochemical records of ODP sites 967 and 968. Newsletters Stratigr. 47 (3), 263–282.
Kroon, D., Alexander, I., Little, M., Lourens, L.J., Matthewson, A., Robertson, A.H., Sakamoto, T., 1998. Oxygen isotope and sapropel stratigraphy in the eastern Mediterranean during the last 3.2 million years. In: Proceedings of the Ocean Drilling Program, Scientific Results, vol. 160.
Laskar, J., Joutel, F., Boudin, F., 1993. Orbital, precessional, and insolation quantities for the earth from −20 MYR to 10 MYR. Astron. Astrophys. 270, 522–533.
Lemieux-Dudon, B., Blayo, E., Petit, J., Waelbroeck, C., Svensson, A., Ritz, C., Barnola, J., Narcisi, B.M., Parrenin, F., 2010. Consistent dating for Antarctic and Greenland ice cores. Quat. Sci. Rev. 29, 8–20.
Lisiecki, L.E., Raymo, M.E., 2005. A Pliocene-Pleistocene stack of 57 globally distributed benthic $\delta^{18}O$ records. Paleoceanography 20, PA1003.
Lisiecki, L.E., Raymo, M.E., 2009. Diachronous benthic $\delta^{18}O$ responses during late Pleistocene terminations. Paleoceanography 24, PA3210.
Lourens, L.J., 2004. Revised tuning of Ocean Drilling Program Site 964 and KC01B (Mediterranean) and implications for the $\delta^{18}O$, tephra, calcareous nannofossil, and geomagnetic reversal chronologies of the past 1.1 Myr. Paleoceanography 19, PA3010.
Lourens, L.J., Wehausen, R., Brumsack, H., 2001. Geological constraints on tidal dissipation and dynamical ellipticity of the earth over the past three million years. Nature 409, 1029–1033.
Lourens, L.J., Antonarakou, A., Hilgen, F., Van Hoof, A., Vergnaud-Grazzini, C., Zachariasse, W., 1996. Evaluation of the Plio-Pleistocene astronomical timescale. Paleoceanography 11, 391–413.
Lourens, L.J., Becker, J., Bintanja, R., Hilgen, F.J., Tuenter, E., van de Wal, R.S.W., Ziegler, M., 2010. Linear and non-linear response of Late Neogene glacial cycles to obliquity forcing and implications for the Milankovitch theory. Quat. Sci. Rev. 29, 352–365.
Martrat, B., Grimalt, J.O., Lopez-Martinez, C., Cacho, I., Sierro, F.J., Flores, J.A., Zahn, R., Canals, M., Curtis, J.H., Hodell, D.A., 2004. Abrupt temperature changes in the Western Mediterranean over the past 250,000 years. Science (New York, N.Y.) 306, 1762–1765.
Maslin, M.A., Ridgewell, A.J., 2005. Mid-Pleistocene revolution and the 'eccentricity myth'. In: Geological Society London Special Publications, vol. 247, pp. 19–34.
Mudelsee, M., Stattegger, K., 1997. Exploring the structure of the mid-pleistocene revolution with advanced methods of time-series analysis. Geol. Rundsch. 86, 499–511.
Mudelsee, M., Schulz, M., 1997. The mid-pleistocene climate transition: onset of 100 ka cycle lags ice volume build-up by 280 ka. Earth Planet. Sci. Lett. 151, 117–123.
Paillard, D., Labeyrie, L., Yiou, P., 1996. Macintosh program performs time-series analysis. Eos Trans. Am. Geophys. Union 77, 379.
Parrenin, F., Barnola, J., Beer, J., Blunier, T., Castellano, E., Chappellaz, J., Dreyfus, G., Fischer, H., Fujita, S., Jouzel, J., 2007. The EDC3 chronology for the EPICA dome C ice core. Clim. Past 3, 485–497.
Raymo, M., 1997. The timing of major climate terminations. Paleoceanography 12, 577–585.
Robinson, A.R., Malanotte-Rizzoli, P., Hecht, A., Michelato, A., Roether, W., Theocharis, A., Ünlüata, Ü., Pinardi, N., Artegiani, A., Bergamasco, A., 1992. General circulation of the Eastern Mediterranean. Earth-Sci. Rev. 32, 285–309.
Rohling, E., Grant, K., Bolshaw, M., Roberts, A., Siddall, M., Hemleben, C., Kucera, M., 2009. Antarctic temperature and global sea level closely coupled over the past five glacial cycles. Nat. Geosci. 2, 500–504.
Rohling, E.J., Foster, G.L., Grant, K.M., Marino, G., Roberts, A.P., Tamisiea, M.E., Williams, F., 2014. Sea-level and deep-sea-temperature variability over the past 5.3 million years. Nature 508, 477–482.
Rohling, E.J., 1999. Environmental control on Mediterranean salinity and $\delta^{18}O$. Paleoceanography 14, 706–715.
Rossignol-Strick, M., 1985. Mediterranean quaternary sapropels, an immediate response of the African monsoon to variation of insolation. Palaeogeogr. Palaeoclimatol. Palaeoecol. 49, 237–263.
Sakamoto, T., Janecek, T., Emeis, K.-C., 1998. Continuous sedimentary sequences from the eastern Mediterranean Sea: composite depth sections. Proceedings of the Ocean Drilling Program. Scientific results vol. 160, 37–59.
Shackleton, N., Berger, A., Peltier, W., 1990. An alternative astronomical calibration of the Lower Pleistocene timescale based on ODP site 677. Trans. R. Soc. Edinb. Earth Sci. 81, 251–261.
Shackleton, N.J., 1995. New data on the evolution of Pliocene climate variability. In: Vrba, E.S., et al. (Eds.), Paleoclimate and Evolution, with Emphasis on Human Origins. Yale Univ. Press, New Haven, Ct, pp. 242–248.
Siddall, M., Rohling, E.J., Almogi-Labin, A., Hemleben, C., Meischner, D., Schmelzer, I., Smeed, D., 2003. Sea-level fluctuations during the last glacial cycle. Nature 423, 853–858.
Skinner, L., Shackleton, N., 2005. An Atlantic lead over Pacific deep-water change across termination I: Implications for the application of the marine isotope stage stratigraphy. Quat. Sci. Rev. 24, 571–580.
Tiedemann, R., Sarnthein, M., Shackleton, N.J., 1994. Astronomic timescale for the Pliocene Atlantic $\delta^{18}O$ and dust flux records of ocean drilling program site 659. Paleoceanography 9, 619–638.
Torrence, C., Compo, G.P., 1998. A practical guide to wavelet analysis. Bull. Am. Meteorol. Soc. 79, 61–78.
Tzedakis, P., 2007. Seven ambiguities in the Mediterranean palaeoenvironmental narrative. Quat. Sci. Rev. 26, 2042–2066.
Wang, Y., Cheng, H., Edwards, R.L., Kong, X., Shao, X., Chen, S., Wu, J., Jiang, X., Wang, X., An, Z., 2008. Millennial- and orbital-scale changes in the East Asian monsoon over the past 224,000 years. Nature 451, 1090–1093.
Wehausen, R., Brumsack, H., 2000. Chemical cycles in Pliocene sapropel-bearing and sapropel-barren Eastern Mediterranean sediments. Palaeogeogr. Palaeoclimatol. Palaeoecol. 158, 325–352.
Wolff, E.W., Fischer, H., Fundel, F., Ruth, U., Twarloh, B., Littot, G.C., Mulvaney, R., Röthlisberger, R., De Angelis, M., Boutron, C.F., 2006. Southern ocean sea-ice extent, productivity and iron flux over the past eight glacial cycles. Nature 440, 491–496.
Ziegler, M., Tuenter, E., Lourens, L.J., 2010. The precession phase of the boreal summer monsoon as viewed from the Eastern Mediterranean (ODP site 968). Quat. Sci. Rev. 29, 1481–1490.